Dynamic event-triggered networked predictive control for discrete-time NCSs under deception attacks

Wu, Zhiying; Wang, Zhe; Wang, Yan; Xiong, Junlin; Xie, Min

Published in:
International Journal of Robust and Nonlinear Control

Online published: 12/12/2022

Document Version:
Post-print, also known as Accepted Author Manuscript, Peer-reviewed or Author Final version

Publication record in CityU Scholars:
Go to record

Published version (DOI):
10.1002/rnc.6535

Publication details:
Wu, Z., Wang, Z., Wang, Y., Xiong, J., & Xie, M. (2022). Dynamic event-triggered networked predictive control for discrete-time NCSs under deception attacks. *International Journal of Robust and Nonlinear Control*. Advance online publication. https://doi.org/10.1002/rnc.6535

Dynamic event-triggered networked predictive control for discrete-time NCSs under deception attacks *

Zhiying Wu† Zhe Wang‡ Yan Wang§ Junlin Xiong¶ Min Xie‖

Abstract

This paper investigates the dynamic event-triggered predictive control problem for discrete-time networked control systems under deception attacks. A new dynamic event-triggered scheme is proposed for discrete-time networked predictive control systems to reduce the data transmission. The feature of the dynamic event-triggered scheme is that the triggering threshold is adjusted dynamically. The Luenberger observer is provided to estimate the output measurements. The networked predictive control method is used to compensate for the time delay. Next, by using the piecewise linear model and the augmented model methods, sufficient conditions are established to guarantee the mean square asymptotic stability of the closed-loop systems, respectively. Finally, the effectiveness of the proposed approach is validated via a buck DC-DC converter system.

Keywords: Deception attacks, dynamic event-triggered scheme, networked predictive control (NPC), time delay.

1 Introduction

Networked control systems (NCSs) are a type of systems, wherein the system components are connected by network [1, 2, 3, 4, 5]. NCSs have been applied in many practical systems: unmanned aerial vehicles systems [6, 7], and power systems [8, 9]. The unreliability of the communication network may lead to packet dropouts, time delays and other unavoidable problems. Because of these factors, the control performance of NCSs may deteriorate, and even the whole system will become unstable. To compensate for time delays and packet dropouts, the networked predictive control (NPC) method was proposed [10]. By using NPC method, the control performance can be maintained. The NPC method is widely applied in NCSs. In particular, the networked predictive control systems is analyzed in [11] via cloud computing. By using NPC method, time delays can be compensated, and the system stability can be maintained. However, most of the results are derived under the time-triggered scheme (TTS) [12, 13, 14, 15, 16]. The TTS may lead to the waste of communication resources.

Event-triggered schemes (ETSs) reduce the transmission rate while achieving the control performance [17, 18, 19, 20, 21]. The measurements are transmitted when the conditions of ETSs are satisfied. Lately, event-triggered predictive control begins to gain attention [22, 23, 24]. For example, the event-triggered predictive control problem is investigated in [22]. However, the maximum inter-event interval is required to be given

*The work described in this paper was supported by the InnoHK program, National Natural Science Foundation of China (71971181, 72032005, and 61773357), and also by Research Grant Council of Hong Kong, Hong Kong ITC/CIMDA and City University of Hong Kong (under grants Nos. 11203519, 11200621 and 9360163) (Corresponding author: Yan Wang.).

†Zhiying Wu is with the Centre for Artificial Intelligence & Robotics, Hong Kong Institute of Science & Innovation, Chinese Academy of Sciences, Hong Kong, and also with Department of Advanced Design and Systems Engineering, City University of Hong Kong, Kowloon, Hong Kong. Email: wzy100@mail.ustc.edu.cn

‡Zhe Wang is with the Center for Intelligent Multidimensional Data Analysis, Hong Kong Science Park, Shatin, Hong Kong. Email: mr.zhe.wang@outlook.com.

§Yan Wang is with the Department of Computing, The Hong Kong Polytechnic University, Kowloon, Hong Kong. Email: wangyany@mail.ustc.edu.cn.

¶Junlin Xiong is with Department of Automation, University of Science and Technology of China, Hefei, China. Email:xiong77@ustc.edu.cn.

‖Min Xie is with the Department of Advanced Design and Systems Engineering, City University of Hong Kong, Kowloon, Hong Kong, and also with the Center for Intelligent Multidimensional Data Analysis, Hong Kong Science Park, Shatin, Hong Kong. Email: minxie@cityu.edu.hk.

in advance in [22], which is inapplicable in practice. To overcome this problem, the piecewise linear model (PWL) and the augmented model approaches are used in [23]. Based on the results in [23], the event-triggered predictive control problem is studied in [24] subject to two-channel delays. However, the above results are established under the static ETSs. To further reduce the transmission rate, dynamic ETSs have been proposed by using additional dynamic variables. In particular, dynamic ETSs have been investigated for NCSs in [25, 26, 27, 28]. Under the dynamic ETSs, the transmission rate is reduced. Meanwhile, the control performance can be similar with that under the static forms. Therefore, it is meaningful to investigate the NPC problem for NCSs based on the dynamic ETS.

On the other hand, the communication channels are vulnerable to be attacked in NCSs. Cyber attacks may damage the control performance, and even destroy system stability [29, 30, 31, 32, 33]. Among the cyber attacks, the deception attacks is one of the important attacks. The attackers replace the measurements with malicious signals, which severely damages the network security. The control problems under deception attacks have attracted substantial attention [34, 35, 36, 37, 38]. In particular, the resilient event-triggered control problem is investigated in [34] subject to deception attacks. The event-triggered load frequency control under problem is investigated in [35] subject to deception attacks and denial-of-service attacks. The memory-based event-triggered control problem is addressed in [36] for NCSs subject to deception attacks. The event-triggered NPC problem is studied in [37] under DoS attacks. However, the deception attack problem has not been explored for the event-triggered predictive control of NCSs.

Motivated by above discussions, it is significant and challenging to propose a framework of the dynamic ETS and the NPC method to deal with time delays and deception attacks. The two main difficulties need to be overcome: Firstly, how to choose the Lyapunov function for discrete-time NCSs based on the dynamic ETS to guarantee the NPC system stability; Secondly, how to construct the NPC system model under the deception attacks. The approaches in [22, 23, 24, 36, 37] are not applicable to the problem studied in this paper, because the results of [22, 23, 24, 37] are just based on static ETSs, and the event-triggered predictive control framework is not considered in [36]. The main contributions of this paper are summarized as follows:

1) The NPC problem is, for the first time, investigated for *discrete-time* NCSs under dynamic ETS and deception attacks. A dynamic ETS is proposed for *discrete-time* networked predictive control systems to reduce the transmission rate compared with the static ETS in [23].

2) A new system model is established, which contains stochastic deception attacks, time delays, and dynamic ETS in a unified framework.

3) New Lyapunov functions are constructed based on the PWL model and the augmented model approaches.

The rest of this paper is as follows. In Section 2, the problem are formulated. In Section 3, the PWL model and the augmented model approaches are presented. Moreover, by using above mentioned two methods, sufficient conditions are derived in terms of linear matrix inequalities (LMIs), respectively. In Section 4, a buck DC-DC converter system is exploited to show the validity of the proposed approaches. In Section 5, the paper is concluded.

Notation: X^T denotes the transposition of matrix X. $X > 0$ ($X < 0$) denotes a positive (negative) definite matrix. $\mathbb{R}^n$ represents the n-dimensional Euclidean space. $\lambda_{\min}(X)$ denotes the minimum eigenvalue of matrix X. $||x|| := \sqrt{x^T x}$ denotes 2-norm of x. $\text{col}\{x_1, \ldots, x_{n_x}\}$ denotes $[x_1^T, \ldots, x_{n_x}^T]^T$. "$\star$" represents the symmetric matrix entry.

2 Problem formulation

Consider the discrete-time linear system as follows:

$$\begin{cases} x_{k+1} = Ax_k + Bu_k, \\ y_k = Cx_k, \end{cases} \tag{1}$$

where $x_k \in \mathbb{R}^{n_x}$ denotes the system state, $u_k \in \mathbb{R}^m$ denotes the system input, and $y_k \in \mathbb{R}^{n_y}$ is the measured output. The framework of the investigated NCS is illustrated in Fig. 1. To reduce communication resources,

a dynamic ETS is proposed. Under the dynamic ETS, the measured outputs are sent over the networks subject to deception attacks. The assumptions are stated as follows.

Assumption 1 *[23] The pairs (A, C) and (A, B) are observable and controllable, respectively.*

Assumption 2 *[23] The constant delay d between the communication channel is considered in this paper. In addition, a time stamp is added to the transmitted signals.*

2.1 Dynamic ETS

To reduce the transmission rate, a dynamic ETS is proposed as follows:

$$\text{ETS}: \ \bar{y}_k = y_k, \ \text{if } \vartheta E(k) > \rho(k), \tag{2}$$

where $\vartheta > 0$ is a scalar, $E(k) = (y_k - \bar{y}_{k-1})^T(y_k - \bar{y}_{k-1}) - \delta^2 y_k^T y_k$ with $0 < \delta < 1$, $\bar{y}_{k-1}$ denotes the latest transmitted signal, $\bar{y}_k$ denotes the current transmitted signal, and y_k is the current measured output. Similar with the definition in [25], $\rho(k)$ is an additional dynamic variable satisfying the following difference equations:

$$\rho(k+1) = \mu\rho(k) - E(k), \ \rho(0) = \rho^0, \tag{3}$$

where $\rho^0 \geq 0$ is the initial condition of the dynamic variable $\rho(k)$, $0 < \mu < 1$, and $\vartheta \geq \frac{1}{\mu}$ are scalars.

Then, if the condition of the dynamic ETS (2) isn't satisfied, the last transmitted signal $\bar{y}_{k-1}$ is transmitted to the observer at k time instant. Thus, we have

$$\bar{y}_k = \bar{y}_{k-1}, \ \text{when } \vartheta E(k) \leq \rho(k). \tag{4}$$

Remark 1 *The dynamic variable $\rho(k)$ can be considered as a filtered value of $-E(k)$. By removing the dynamic variable $\rho(k)$, the dynamic ETS (2) is reduced into the static ETS in [23], which is given by*

$$ETS: \ \bar{y}_k = y_k, \ \textit{if } E(k) > 0. \tag{5}$$

Therefore, when $\vartheta \to \infty$, the dynamic ETS (2) becomes the static ETS (5). Moreover, the parameters δ and μ in (2) are important for the proposed dynamic ETS. By adjusting the dynamic parameters δ and μ, the dynamic ETS (2) can further reduce the transmission rate. The larger the triggered parameter δ, the smaller the transmission rate becomes. The number of data transmission is larger with the increasing μ. This advantage will be proved in the later section, see Lemma 1 in the next section, Tables 2 and 3 in the example section. From (2), the inter-event interval of the dynamic ETS is not smaller than the sampling period h, because discrete-time NCSs are investigated. Thus, the Zeno phenomenon is avoided.

2.2 System modeling under stochastic deception attacks

Similar to the modeling of stochastic deception attacks in [36], assume that the adversary can capture and replace the output $\bar{y}_k$ by malicious signal $g(\bar{y}_k)$ randomly.

Considering the stochastic deception attacks, the real signals that transmitting at controller are reformed as

$$y_k^r = \beta_k g(\bar{y}_k) + (1 - \beta_k)\bar{y}_k, \tag{6}$$

where $\beta_k \in \{0, 1\}$ is a Bernoulli stochastic variable, which describes the stochastic features of deception attacks. To be specific, if $\beta_k = 0$, then $y_r = \bar{y}_k$, i.e., there are no deception attacks. On the other hand, when $\beta_k = 1$, then the received signal y_r is the malicious signal $g(\bar{y}_k)$. Moreover, assume that

$$\mathbb{E}\{\beta_k\} = \bar{\beta}, \ \mathbb{E}\{(\beta_k - \bar{\beta})^2\} = \lambda^2, \tag{7}$$

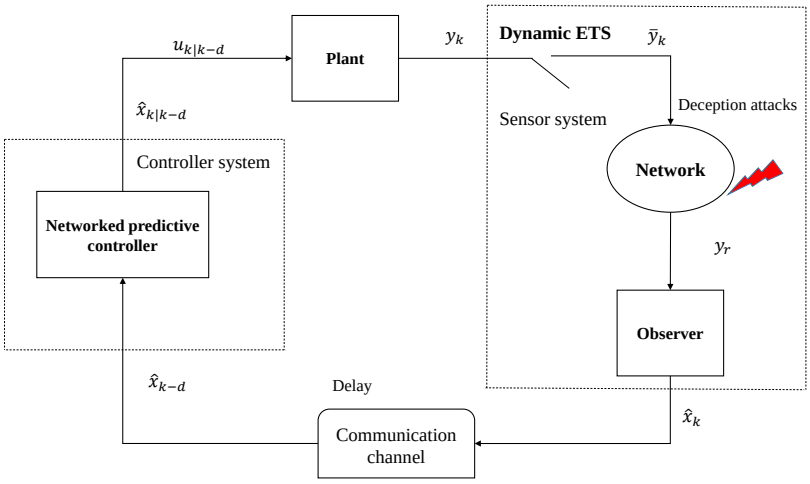

Fig. 1: Event-triggered NPC system.

where $\lambda = \sqrt{\bar{\beta}(1-\bar{\beta})}$.

In practice, the full information of system states is usually unavailable. From the received signal y_r, the Luenberger observer is constructed as follows:

$$\begin{cases} \hat{x}_{k+1} = A\hat{x}_k + Bu_k + L(y_k^r - \hat{y}_k), \\ \hat{y}_k = C\hat{x}_k, \end{cases} \tag{8}$$

where $\hat{x}_k \in \mathbb{R}^{n_x}$ and $\hat{y}_k \in \mathbb{R}^{n_y}$ are the observer state and the observer output, respectively, and L is the observer gain matrix.

In the NCS, the time-delay is unavoidable. To compensate for the time delay, the NPC method is proposed. Firstly, the state predictions from time instant $k-d+1$ to time instant k are given by

$$\begin{aligned} \hat{x}_{k-d+1} &= A\hat{x}_{k-d} + Bu_{k-d} + L(y_{k-d}^r - \hat{y}_{k-d}), \\ \hat{x}_{k-d+2|k-d} &= A\hat{x}_{k-d+1} + Bu_{k-d+1}, \\ &\vdots \\ \hat{x}_{k|k-d} &= A\hat{x}_{k-1} + Bu_{k-1}, \end{aligned} \tag{9}$$

where $\hat{x}_{k-d+i|k-d}$, $(i = 2, 3, \cdots, d,)$ is the state prediction at time instant $k-d+i$ based on the information at $k-d$. From (9), we have

$$\hat{x}_{k|k-d} = A^{d-1}\hat{x}_{k-d+1} + \sum_{i=2}^{d} A^{d-i}Bu_{k+i-d-1}, \tag{10}$$

where $\hat{x}_{k-d+1|k-d} = \hat{x}_{k-d+1}$ is a one-step prediction of the state. Thus, the control prediction is described as

$$u_k = K\hat{x}_{k|k-d}, \tag{11}$$

where K is the controller gain.

Remark 2 *In the existing works, the unified framework of the NPC method, the ETS and deception attacks hasn't been proposed for NCSs. In this paper, a new system model is proposed, which covers the NPC method, stochastic deception attacks, and dynamic ETS in a unified framework. If time-delay is also considered in dynamic ETS, i.e., two-channel delays are considered, the results in this paper can be directly extended by using the methods in [24]. Compared with the static ETSs in [23, 24, 39], the dynamic ETS* (2) *can further reduce the transmission rate. Moreover, the works in [23, 24, 40] don't consider the system under cyber attack, which is vulnerable in practice.*

2.3 Problem statement

Before stating the problem to be investigated in this paper, the following assumption and definition are introduced.

Assumption 3 *[36] To restrict the deception attacks, the following condition needs to be satisfied:*

$$||G\bar{y}_k||^2 \geq ||g(\bar{y}_k)||^2 \tag{12}$$

where G is a constant matrix.

Definition 1 *[41] The investigated system is said to be asymptotically stable in the mean-square sense if $\lim_{t\to\infty} \mathbb{E}[||x(t)||^2] = 0$ for any initial condition $x(0)$.*

In the paper, the objective is to guarantee the mean-square asymptotic stability for the dynamic event-triggered control system.

3 Dynamic event-triggered predictive control

In this section, a lemma is presented to analyze the dynamic variable $\rho(k)$. Next, the stability of the event-triggered predictive control system is guaranteed by using two different techniques: the augmented model and the PWL model, respectively.

Lemma 1 *In the dynamic ETS (2), $\rho(k) \geq 0$ for all $k \in \mathbb{N}_0$.*

Proof. From (2), we have

$$E(k) \leq \frac{1}{\vartheta}\rho(k). \tag{13}$$

It follows from (3) that

$$\begin{aligned}\rho(k+1) &\geq (\mu - \frac{1}{\vartheta})\rho(k) \geq (\mu - \frac{1}{\vartheta})^2\rho(k-1) \\ &\geq \ldots \geq (\mu - \frac{1}{\vartheta})^{k+1}\rho(0) \geq 0.\end{aligned} \tag{14}$$

The proof is completed. ■

3.1 Augmented Model

Let $e_k = y_k - \bar{y}_k$, and $\tilde{x}_k = x_k - \hat{x}_k$. From (1) and (9), we obtain

$$\begin{aligned}&x_k - \hat{x}_{k|k-d} \\ &= A(x_{k-1} - \hat{x}_{k-1|k-d}) \\ &\quad \vdots \quad \vdots \quad \vdots \\ &= A^{d-1}(x_{k-d+1} - \hat{x}_{k-d+1|k-d}) \\ &= A^d(x_{k-d} - \hat{x}_{k-d}) - A^{d-1}L\{[\beta_{k-d}g(\bar{y}_{k-d}) \\ &\quad + (1-\beta_{k-d})(Cx_{k-d} - e_{k-d})] - C\hat{x}_{k-d}\} \\ &= [A^d - (1-\beta_{k-d})A^{d-1}LC]x_{k-d} - [A^d - A^{d-1}LC]\hat{x}_{k-d} \\ &\quad - \beta_{k-d}A^{d-1}Lg(\bar{y}_{k-d}) + (1-\beta_{k-d})A^{d-1}Le_{k-d}.\end{aligned} \tag{15}$$

It follows from (11) that

$$\begin{aligned} x_{k+1} &= Ax_k + BK\hat{x}_{k|k-d} \\ &= (A+BK)x_k - BK(x_k - \hat{x}_{k|k-d}) \\ &= (A+BK)x_k - BK[A^d - (1-\beta_{k-d})A^{d-1}LC]x_{k-d} \\ &\quad + BK[A^d - A^{d-1}LC]\hat{x}_{k-d} + \beta_{k-d}BKA^{d-1}Lg(\bar{y}_{k-d}) \\ &\quad - (1-\beta_{k-d})BKA^{d-1}Le_{k-d}. \end{aligned} \tag{16}$$

Furthermore, the state and the estimated state are calculated as follows:

$$\begin{aligned} x_{k-d+1} &= Ax_{k-d} + Bu_{k-d} \\ &= Ax_{k-d} + BK\hat{x}_{k-d}, \end{aligned} \tag{17}$$

$$\begin{aligned} \hat{x}_{k-d+1} &= A\hat{x}_{k-d} + Bu_{k-d} + L\{[\beta_{k-d}g(\bar{y}_{k-d}) \\ &\quad + (1-\beta_{k-d})(Cx_{k-d} - e_{k-d})] - C\hat{x}_{k-d}\} \\ &= (1-\beta_{k-d})LCx_{k-d} + (A+BK-LC)\hat{x}_{k-d}) \\ &\quad + \beta_{k-d}Lg(\bar{y}_{k-d}) - (1-\beta_{k-d})Le_{k-d}. \end{aligned} \tag{18}$$

Let $\eta_k \triangleq \text{col}\{x_k, x_{k-d}, \hat{x}_{k-d}\}$. Then, the augmented system model is presented as follows:

$$\begin{cases} \eta_{k+1} = \mathcal{A}\eta_k + \mathcal{B}g(\bar{y}_{k-d}) + \mathcal{L}e_{k-d}, \\ e_{k-d} = \mathcal{E}_2\eta_k - \bar{y}_{k-d}, \end{cases} \tag{19}$$

where

$$\begin{aligned} \mathcal{A} &= \begin{bmatrix} A+BK & \mathcal{A}_{12} & BK[A^d - A^{d-1}LC] \\ 0 & A & BK \\ 0 & (1-\beta_{k-d})LC & A+BK-LC \end{bmatrix}, \\ \mathcal{B} &= \begin{bmatrix} \beta_{k-d}BKA^{d-1}L \\ 0 \\ \beta_{k-d}L \end{bmatrix}, \ \mathcal{L} = \begin{bmatrix} -(1-\beta_{k-d})BKA^{d-1}L \\ 0 \\ -(1-\beta_{k-d})L \end{bmatrix}, \\ \mathcal{E}_2 &= \begin{bmatrix} 0 & C & 0 \end{bmatrix}, \ \mathcal{A}_{12} = -BK[A^d - (1-\beta_{k-d})A^{d-1}LC]. \end{aligned}$$

Next, the following theorem is derived for ensuring the system stability.

3.2 Stability analysis

Theorem 1 *For given matrices K and L, and given scalars d, $0 < \delta < 1$ and $0 < \mu < 1$, if there exist a scalar $\epsilon > 0$, and matrices $P > 0$, $S > 0$ and $R > 0$ such that*

$$\Theta = \begin{bmatrix} \Theta_{11} & \Theta_{12} & \Theta_{13} & 0 & 0 \\ * & \Theta_{22} & \Theta_{23} & 0 & 0 \\ * & * & \Theta_{33} & 0 & -G^TGC \\ * & * & * & S-I & 0 \\ * & * & * & * & \Theta_{55} \end{bmatrix} < 0 \tag{20}$$

where

$$\begin{aligned} \Theta_{11} &= \lambda^2\bar{\mathcal{A}}^TP\bar{\mathcal{A}} + \hat{\mathcal{A}}^TP\hat{\mathcal{A}} + \mathcal{C} - P + \epsilon I, \\ \Theta_{12} &= \lambda^2\bar{\mathcal{A}}^TP\bar{\mathcal{B}} + \hat{\mathcal{A}}^TP\hat{\mathcal{B}}, \\ \Theta_{13} &= \lambda^2\bar{\mathcal{A}}^TP\bar{\mathcal{L}} + \hat{\mathcal{A}}^TP\hat{\mathcal{L}}, \\ \Theta_{22} &= \lambda^2\bar{\mathcal{B}}^TP\bar{\mathcal{B}} + \hat{\mathcal{B}}^TP\hat{\mathcal{B}} - I, \\ \Theta_{23} &= \lambda^2\bar{\mathcal{B}}^TP\bar{\mathcal{L}} + \hat{\mathcal{B}}^TP\hat{\mathcal{L}}, \end{aligned}$$

$$
\begin{aligned}
\Theta_{33} &= \lambda^2 \bar{\mathcal{L}}^T P \bar{\mathcal{L}} + \hat{\mathcal{L}}^T P \hat{\mathcal{L}} - S, \\
\Theta_{55} &= -R + C^T G^T G C, \\
\mathcal{C} &= \begin{bmatrix} \delta^2 C^T C + R & 0 \\ 0 & 0 \end{bmatrix}, \ \bar{\mathcal{A}} = \begin{bmatrix} 0 & -BKA^{d-1}LC \\ 0 & LC \end{bmatrix}, \\
\hat{\mathcal{A}} &= \begin{bmatrix} A + BK & -BK[A^d - (1-\bar{\beta})A^{d-1}LC] \\ 0 & A - (1-\bar{\beta})LC \end{bmatrix}, \\
\bar{\mathcal{B}} &= \begin{bmatrix} BKA^{d-1}L \\ -L \end{bmatrix}, \ \hat{\mathcal{B}} = \begin{bmatrix} \bar{\beta}BKA^{d-1}L \\ -\bar{\beta}L \end{bmatrix}, \\
\bar{\mathcal{L}} &= \begin{bmatrix} BKA^{d-1}L \\ -L \end{bmatrix}, \ \hat{\mathcal{L}} = \begin{bmatrix} -(1-\bar{\beta})BKA^{d-1}L \\ (1-\bar{\beta})L \end{bmatrix}.
\end{aligned}
$$

then the investigated system (19) *is mean square asymptotically stable.*

Proof. Construct the Lyapunov function as follows:

$$
V(k) = \sum_{i=1}^{3} V_i(k) + \rho(k), \text{ for } k \geq 0 \tag{21}
$$

where

$$
\begin{cases}
V_1(k) = \eta_k^T P \eta_k, \\
V_2(k) = \sum_{i=k-d}^{k-1} x_i^T R x_i, \\
V_3(k) = \sum_{i=k-d}^{k-1} e_i^T S e_i,
\end{cases}
$$

with $P > 0$, $R > 0$ and $S > 0$.

From Lemma 1, we have $\rho(k) \geq 0$. Therefore, we obtain

$$
\begin{aligned}
&\mathbb{E}\{\Delta V(k)\} = \mathbb{E}\{\sum_{i=1}^{3} \Delta V_i(k) + \Delta\rho(k)\} \\
&= \mathbb{E}\{\eta_{k+1}^T P \eta_{k+1}\} - \eta_k^T P \eta_k + x_k^T R x_k - x_{k-d}^T R x_{k-d} \\
&\quad + e_k^T S e_k - e_{k-d}^T S e_{k-d} + (\mu - 1)\rho(k) - E(k) \\
&\leq \mathbb{E}\{\eta_{k+1}^T P \eta_{k+1}\} - \eta_k^T P \eta_k + x_k^T R x_k - x_{k-d}^T R x_{k-d} \\
&\quad + e_k^T S e_k - e_{k-d}^T S e_{k-d} + \delta^2 x_k^T C^T C x_k - e_k^T e_k.
\end{aligned} \tag{22}
$$

Note that $\eta_{k+1} = [(\beta_{k-d} - \bar{\beta})\bar{\rho}_s + \hat{\rho}_s]\phi$, where $\bar{\rho}_s = \begin{bmatrix} \bar{\mathcal{A}} & \bar{\mathcal{B}} & \bar{\mathcal{L}} & 0 & 0 \end{bmatrix}$, $\hat{\rho}_s = \begin{bmatrix} \hat{\mathcal{A}} & \hat{\mathcal{B}} & \hat{\mathcal{L}} & 0 & 0 \end{bmatrix}$, and augmented vector $\phi = \text{col}\{\eta_k, g(\bar{y}_{k-d}), e_{k-d}, e_k, x_{k-d}\}$. Hence, we have

$$
\mathbb{E}\left\{\eta_{k+1}^T P \eta_{k+1}\right\} = \lambda^2 \phi^T \bar{\rho}_s^T P \bar{\rho}_s \phi + \phi^T \hat{\rho}_s^T P \hat{\rho}_s \phi \tag{23}
$$

where the properties $\mathbb{E}\{(\beta_{k-d} - \bar{\beta})^2\} = \lambda^2$, and $\mathbb{E}\{\beta_{k-d} - \bar{\beta}\} = 0$ are used.

Based on Assumption 3, we have

$$
\begin{aligned}
g^T(\bar{y}_{k-d}) g(\bar{y}_{k-d}) &\leq \bar{y}_{k-d}^T G^T G \bar{y}_{k-d} \\
&= (Cx_{k-d} - e_{k-d})^T G^T G (Cx_{k-d} - e_{k-d}).
\end{aligned}
$$

Thus, we obtain

$$
\begin{aligned}
\mathbb{E}\{\Delta V(k)\} &\leq \mathbb{E}\{\Delta V(k)\} - g^T(\bar{y}_{k-d}) g(\bar{y}_{k-d}) \\
&\quad + (Cx_{k-d} - e_{k-d})^T G^T G (Cx_{k-d} - e_{k-d}) \\
&= \phi^T \bar{\Theta} \phi,
\end{aligned} \tag{24}
$$

where $\bar{\Theta} = \begin{bmatrix} \bar{\Theta}_{11} & \Theta_{12} & \Theta_{13} & 0 & 0 \\ * & \Theta_{22} & \Theta_{23} & 0 & 0 \\ * & * & \Theta_{33} & 0 & -G^TGC \\ * & * & * & S-I & 0 \\ * & * & * & * & \Theta_{55} \end{bmatrix}$ with $\bar{\Theta}_{11} = \Theta_{11} - \epsilon I$.

From (20), we have

$$\phi^T \bar{\Theta} \phi \leq -\epsilon \eta_k^T \eta_k < 0, \tag{25}$$

for any $\eta_k \neq 0$. Thus, we obtain

$$\mathbb{E}\{\Delta V(k)\} \leq -\epsilon \eta_k^T \eta_k < 0. \tag{26}$$

Therefore, the investigated system (19) is mean square asymptotically stable. This completes the proof. ■

Remark 3 *Compared with the Lyapunov functions in [23], Lyapunov function in this paper adds a summation term $\sum_{i=k-d}^{k-1} x_i^T R x_i$ to compensate the malicious signal due to the deception attack. Due to the constraint of deception attacks, the summation term $\sum_{i=k-d}^{k-1} x_i^T R x_i$ is included in the augmented vector $\phi = \text{col}\{\eta_k, g(\bar{y}_{k-d}), e_{k-d}, e_k, x_{k-d}\}$. In addition, compared with the system model in [23], a new augmented system model with $\eta_k \triangleq \text{col}\{x_k, x_{k-d}, \hat{x}_{k-d}\}$ is established in this paper. This is due to the introduction of dynamic ETS, the system model in [23, 37] is not applicable. Moreover, based on the dynamic ETS, the term $\rho(k)$ is added in the Lyapunov function. Because of the term $\rho(k)$, the function $\sum_{i=1}^{3} V_i(k)$ may not be a decreasing function compared with that under the static ETS in [23, 37], see inequalities* (21) *and* (26).

Remark 4 *In the dynamic ETS* (2)*, the parameters μ and δ affect the feasibility of the inequalities in Theorem 1. Because the mean square asymptotical stablity are considered in this paper, the decay rate is not involved for the Lyapunov function and exponential stability. Moreover, the parameters ϑ and ρ^0 is independent of the feasibility of the inequalities, but affect the transmission rate and the control performance. Compared with the trigger parameters in [23], the limitation of the dynamic ETS* (2) *is reduced.*

3.3 Piecewise Linear Model

In this subsection, the investigated system stability is analyzed by the PWL model approach.

Let $\bar{\eta}_k \triangleq \text{col}\{x_k, x_{k-d}, \hat{x}_{k-d}, \bar{y}_{k-1}\}$. Then, the investigated system is obtained as follows:

$$\bar{\eta}_{k+1} = \begin{cases} \mathcal{A}_1 \bar{\eta}_k + \tilde{B} g(\bar{y}_{k-d}) + \tilde{L} e_{k-d}, \text{ for } \vartheta \bar{\eta}_k^T W \bar{\eta}_k > \rho(k), \\ \mathcal{A}_2 \bar{\eta}_k + \tilde{B} g(\bar{y}_{k-d}) + \tilde{L} e_{k-d}, \text{ for } \vartheta \bar{\eta}_k^T W \bar{\eta}_k \leq \rho(k) \end{cases} \tag{27}$$

where

$$\mathcal{A}_1 = \begin{bmatrix} A+BK & \mathcal{A}_1^{(1,2)} & BK[A^d - A^{d-1}LC] & 0 \\ 0 & A & BK & 0 \\ 0 & (1-\beta_{k-d})LC & A+BK-LC & 0 \\ C & 0 & 0 & 0 \end{bmatrix},$$

$$\mathcal{A}_2 = \begin{bmatrix} A+BK & \mathcal{A}_2^{(1,2)} & BK[A^d - A^{d-1}LC] & 0 \\ 0 & A & BK & 0 \\ 0 & (1-\beta_{k-d})LC & A+BK-LC & 0 \\ 0 & 0 & 0 & I \end{bmatrix},$$

$$\tilde{B} = \begin{bmatrix} \beta_{k-d} BK A^{d-1} L \\ 0 \\ \beta_{k-d} L \\ 0 \end{bmatrix}, \ \tilde{L} = \begin{bmatrix} -(1-\beta_{k-d}) BK A^{d-1} L \\ 0 \\ -(1-\beta_{k-d}) L \\ 0 \end{bmatrix},$$

$$W = \begin{bmatrix} (1-\delta^2)C^TC & 0 & 0 & -C^T \\ 0 & 0 & 0 & 0 \\ 0 & 0 & 0 & 0 \\ -C & 0 & 0 & I \end{bmatrix},$$

$$\mathcal{A}_1^{(1,2)} = \mathcal{A}_2^{(1,2)} = -BK[A^d - (1-\beta_{k-d})A^{d-1}LC].$$

Remark 5 *Based on the dynamic ETS* (2)*, the system models under the deception attacks are constructed by augmented system model* (19) *and PWL model* (27)*, respectively. A dynamic event-triggered predictive control framework is established, which contains stochastic deception attacks, time delays, and dynamic ETS in a unified framework. The approaches in [22, 23, 24, 36] are not applicable to the problem studied in this paper, because the results of [22, 23, 24, 36] are just based on static ETSs.*

According to the PWL model (27), the result is given as follows.

Theorem 2 *For given matrices K and L, given scalars d, $0 < \delta < 1$ and $0 < \mu < 1$, the mean square asymptotic stability is guaranteed for the investigated system* (27) *if there exist matrices P_1, P_2, $R > 0$, and $S > 0$, and scalars $\xi > 0$, and $\theta_i > 0$, $i, j \in \{1, 2\}$ such that*

$$\begin{bmatrix} \Phi_{11} & \Phi_{12} & \Phi_{13} & 0 \\ * & \Phi_{22} & \Phi_{23} & 0 \\ * & * & \Phi_{33} & -G^T GC \\ * & * & * & \Phi_{44} \end{bmatrix} \leq 0,\ i = 1,\ j \in \{1, 2\}, \tag{28}$$

$$\begin{bmatrix} \bar{\Phi}_{11} & \Phi_{12} & \Phi_{13} & 0 \\ * & \Phi_{22} & \Phi_{23} & 0 \\ * & * & \Phi_{33} & -G^T GC \\ * & * & * & \Phi_{44} \end{bmatrix} \leq 0,\ i = 2,\ j \in \{1, 2\}, \tag{29}$$

$$P_i + (-1)^i \theta_i W > 0,\ i \in \{1, 2\}, \tag{30}$$

where

$$\begin{aligned}
\Phi_{11} &= \lambda^2 \bar{\mathcal{A}}_i^T P_j \bar{\mathcal{A}}_i + \hat{\mathcal{A}}_i^T P_j \hat{\mathcal{A}}_i + \mathcal{R} - P_i + \xi I, \\
\Phi_{12} &= \lambda^2 \bar{\mathcal{A}}_i^T P_j \bar{B} + \hat{\mathcal{A}}_i^T P_j \hat{B}, \\
\Phi_{13} &= \lambda^2 \bar{\mathcal{A}}_i^T P_j \bar{L} + \hat{\mathcal{A}}_i^T P_j \hat{L}, \\
\Phi_{22} &= \lambda^2 \bar{B}^T P_j \bar{B} + \hat{B}^T P_j \hat{B} - I, \\
\Phi_{23} &= \lambda^2 \bar{B}^T P_j \bar{L} + \hat{B}^T P_j \hat{L}, \\
\Phi_{33} &= \lambda^2 \bar{L}^T P_j \bar{L} + \hat{L}^T P_j \hat{L} - S + G^T G, \\
\Phi_{44} &= -R + C^T G^T GC, \\
\bar{\Phi}_{11} &= \Phi_{11} + (\mu - 1) W + Q^T (S - I) Q, \\
Q &= \begin{bmatrix} C & 0 & 0 & -I \end{bmatrix}, \\
\mathcal{R} &= \begin{bmatrix} R + \delta^2 C^T C & 0 & 0 & 0 \\ 0 & 0 & 0 & 0 \\ 0 & 0 & 0 & 0 \\ 0 & 0 & 0 & 0 \end{bmatrix}, \\
\bar{\mathcal{A}}_i &= \begin{bmatrix} 0 & -BKA^{d-1}LC & 0 & 0 \\ 0 & 0 & 0 & 0 \\ 0 & -LC & 0 & 0 \\ 0 & 0 & 0 & 0 \end{bmatrix},\ i = 1, 2, \\
\hat{\mathcal{A}}_1 &= \begin{bmatrix} A + BK & \hat{\mathcal{A}}_1^{(1,2)} & \hat{\mathcal{A}}_1^{(1,3)} & 0 \\ 0 & A & BK & 0 \\ 0 & (1 - \bar{\beta}) LC & A + BK - LC & 0 \\ C & 0 & 0 & 0 \end{bmatrix}, \\
\hat{\mathcal{A}}_2 &= \begin{bmatrix} A + BK & \hat{\mathcal{A}}_2^{(1,2)} & \hat{\mathcal{A}}_2^{(1,3)} & 0 \\ 0 & A & BK & 0 \\ 0 & (1 - \bar{\beta}) LC & A + BK - LC & 0 \\ 0 & 0 & 0 & I \end{bmatrix}, \\
\hat{\mathcal{A}}_i^{(1,2)} &= -BK[A^d - (1 - \bar{\beta}) A^{d-1} LC],\ i = 1, 2, \\
\hat{\mathcal{A}}_i^{(1,3)} &= BK[A^d - A^{d-1} LC],\ i = 1, 2,
\end{aligned}$$

$$\bar{B} = \begin{bmatrix} BKA^{d-1}L \\ 0 \\ -L \\ 0 \end{bmatrix}, \ \hat{B} = \begin{bmatrix} \bar{\beta}BKA^{d-1}L \\ 0 \\ \bar{\beta}L \\ 0 \end{bmatrix}$$

$$\bar{L} = \begin{bmatrix} BKA^{d-1}L \\ 0 \\ L \\ 0 \end{bmatrix}, \ \hat{L} = \begin{bmatrix} -(1-\bar{\beta})BKA^{d-1}L \\ 0 \\ -(1-\bar{\beta})L \\ 0 \end{bmatrix}.$$

Proof. Use the piecewise quadratic Lyapunov function as follows:

$$V(k) = \begin{cases} \bar{\eta}_k^T P_1 \bar{\eta}_k + \sum_{i=k-d}^{k-1} x_i^T R x_i + \sum_{i=k-d}^{k-1} e_i^T S e_i + \rho(k), \\ \text{for } \vartheta \bar{\eta}_k^T W \bar{\eta}_k > \rho(k) \\ \bar{\eta}_k^T P_2 \bar{\eta}_k + \sum_{i=k-d}^{k-1} x_i^T R x_i + \sum_{i=k-d}^{k-1} e_i^T S e_i + \rho(k), \\ \text{for } \vartheta \bar{\eta}_k^T W \bar{\eta}_k \leq \rho(k) \end{cases} \tag{31}$$

To prove $V_k > 0$, it follows from (31) that

$$\begin{aligned} V(k) &= \bar{\eta}_k^T P_1 \bar{\eta}_k + \sum_{i=k-d}^{k-1} x_i^T R x_i + \sum_{i=k-d}^{k-1} e_i^T S e_i + \rho(k) \\ &\geq \bar{\eta}_k^T P_1 \bar{\eta}_k \\ &\geq \lambda_{\min}(P_1 - \theta_1 W)\|\bar{\eta}_k\|^2 + \theta_1 \bar{\eta}_k^T W \bar{\eta}_k \\ &\geq \lambda_{\min}(P_1 - \theta_1 W)\|\bar{\eta}_k\|^2 + \frac{\theta_1}{\vartheta}\rho(k), \\ &\geq \lambda_{\min}(P_1 - \theta_1 W)\|\bar{\eta}_k\|^2 \end{aligned} \tag{32}$$

for all $\bar{\eta}_k$ satisfying $\vartheta \bar{\eta}_k^T W \bar{\eta}_k > \rho(k)$.

Similarly, we have

$$\begin{aligned} V(k) &= \bar{\eta}_k^T P_2 \bar{\eta}_k + \sum_{i=k-d}^{k-1} x_i^T R x_i + \sum_{i=k-d}^{k-1} e_i^T S e_i + \rho(k) \\ &\geq \bar{\eta}_k^T P_2 \bar{\eta}_k + \rho(k) \\ &\geq \lambda_{\min}(P_2 + \theta_2 W)\|\bar{\eta}_k\|^2 - \theta_2 \bar{\eta}_k^T W \bar{\eta}_k + \rho(k) \\ &\geq \lambda_{\min}(P_2 + \theta_2 W)\|\bar{\eta}_k\|^2, \end{aligned} \tag{33}$$

for all $\bar{\eta}_k$ satisfying $\vartheta \bar{\eta}_k^T W \bar{\eta}_k \leq \rho(k)$ and $\theta_2 = \vartheta$. Thus, from (30), we can conclude that there exist scalars $f_1 > 0$ with

$$f_1 = \min\{\lambda_{\min}(P_1 - \theta_1 W), \lambda_{\min}(P_2 + \theta_2 W)\},$$

such that

$$f_1 \|\bar{\eta}_k\|^2 \leq V(k).$$

Thus, $V(k)$ is positive definite. Next, recalling Assumption 3, we obtain

$$\begin{aligned} &\mathbb{E}\{\Delta V(k)\} + \xi\|\bar{\eta}_k\|^2 \\ &= \mathbb{E}\{V(k+1) - V(k)\} + \xi\|\bar{\eta}_k\|^2 \\ &= \mathbb{E}\{\bar{\eta}_{k+1}^T P_j \bar{\eta}_{k+1}\} - \bar{\eta}_k^T P_i \bar{\eta}_k + x_k^T R x_k - x_{k-d}^T R x_{k-d} \\ &\quad + e_k^T S e_k - e_{k-d}^T S e_{k-d} + \rho(k+1) - \rho(k) + \xi\|\bar{\eta}_k\|^2 \\ &= \mathbb{E}\{\bar{\eta}_{k+1}^T P_j \bar{\eta}_{k+1}\} - \bar{\eta}_k^T P_i \bar{\eta}_k + x_k^T R x_k - x_{k-d}^T R x_{k-d} \end{aligned}$$

$$
\begin{aligned}
&+ e_k^T S e_k - e_{k-d}^T S e_{k-d} + (\mu-1)\rho(k) - E(k) + \xi\|\bar{\eta}_k\|^2 \\
&\le \mathbb{E}\{\bar{\eta}_{k+1}^T P_j \bar{\eta}_{k+1}\} - \bar{\eta}_k^T P_i \bar{\eta}_k + x_k^T R x_k - x_{k-d}^T R x_{k-d} \\
&\quad + (Cx_{k-d} - e_{k-d})^T G^T G (Cx_{k-d} - e_{k-d}) - g^T(\bar{y}_{k-d}) g(\bar{y}_{k-d}) \\
&\quad + e_k^T S e_k - e_{k-d}^T S e_{k-d} + \xi\|\bar{\eta}_k\|^2 \\
&\quad + \delta^2 x_k^T C^T C x_k - e_k^T e_k + (\mu-1)\rho(k).
\end{aligned} \tag{34}
$$

Note that $\bar{\eta}_{k+1} = [(\beta_{k-d} - \bar{\beta})\bar{\rho}_t + \hat{\rho}_t]\bar{\phi}$, where $\bar{\rho}_t = \begin{bmatrix}\bar{\mathcal{A}}_i & \bar{B} & \bar{L} & 0\end{bmatrix}$, $\hat{\rho}_t = \begin{bmatrix}\hat{\mathcal{A}}_i & \hat{B} & \hat{L} & 0\end{bmatrix}$ for $i \in \{1,2\}$, and $\bar{\phi} = \mathrm{col}\{\eta_k, g(\bar{y}_{k-d}), e_{k-d}, x_{k-d}\}$. Then, similar with the proof in Theorem 1, we have

$$
\mathbb{E}\left\{\bar{\eta}_{k+1}^T P_j \bar{\eta}_{k+1}\right\} = \lambda^2 \bar{\phi}^T \bar{\rho}_t^T P_j \bar{\rho}_t \bar{\phi} + \bar{\phi}^T \hat{\rho}_t^T P_j \hat{\rho}_t \bar{\phi}, \tag{35}
$$

Based on the definition of $e(k)$, we have

$$
e_k^T (S - I) e_k = \begin{cases} 0, \ i = 1 \\ \bar{\eta}_k^T Q^T (S-I) Q \bar{\eta}_k, \ i = 2 \end{cases} \tag{36}
$$

where Q is defined in (29). Therefore, we obtain

$$
\begin{aligned}
&\mathbb{E}\{\Delta V(k)\} + \xi\|\bar{\eta}_k\|^2 \\
&\le \lambda^2 \bar{\phi}^T \bar{\rho}_t^T P_j \bar{\rho}_t \bar{\phi} + \bar{\phi}^T \hat{\rho}_t^T P_j \hat{\rho}_t \bar{\phi} - \bar{\eta}_k^T P_i \bar{\eta}_k \\
&\quad + e_k^T S e_k - e_{k-d}^T S e_{k-d} + \xi\|\bar{\eta}_k\|^2 + x_k^T R x_k - x_{k-d}^T R x_{k-d} \\
&\quad + \delta^2 x_k^T C^T C x_k - e_k^T e_k + (\mu-1)\rho(k) - g^T(\bar{y}_{k-d}) g(\bar{y}_{k-d}) \\
&\quad + (Cx_{k-d} - e_{k-d})^T G^T G (Cx_{k-d} - e_{k-d}) \\
&\le \begin{cases} 0, \ i = 1 \\ (1-\mu)(\bar{\eta}_k^T W \bar{\eta}_k - \rho(k)), \ i = 2 \end{cases}
\end{aligned} \tag{37}
$$

From (31), it should be noted that when

$$
V(k) = \bar{\eta}_k^T P_2 \bar{\eta}_k + \sum_{i=k-d}^{k-1} x_i^T R x_i + \sum_{i=k-d}^{k-1} e_i^T S e_i, \ i = 2 \tag{38}
$$

there holds that $\bar{\eta}_k^T W \bar{\eta}_k - \rho(k) < 0$. Thus,

$$
\mathbb{E}\{\Delta V(k)\} + \xi\|\bar{\eta}_k\|^2 \le 0. \tag{39}
$$

which indicates that

$$
\mathbb{E}\{\Delta V(k)\} \le -\xi\|\bar{\eta}_k\|^2 < 0. \tag{40}
$$

The proof is completed. ■

Remark 6 *To guarantee the positive definiteness of Lyapunov function, it is required that the trigger parameter $\vartheta = \theta_2$ in the dynamic ETS* (2)*. This constraint is introduced due to the dynamic ETS* (2)*, but the dynamic ETS* (2) *can further reduce the transmission rate. This advantage will be proved in the example section. On the other hand, compared with the PWL model method, less free variables are involved by using the augmented model method, see LMI* (20)*. Thus, the computation is reduced. The augmented model approach is more conservative, compared with the PWL model method. The advantages of the PWL model method are as follows: (i) The dynamic ETS is modelled in the PWL system* (27)*, whereas the augmented model does not contain the inequality constraint* (4)*. (ii) The matrices P_1 and P_2 used in the piecewise Lyapunov function* (31) *is more flexible than the matrix P used in the non-piecewise Lyapunov function* (21)*. Compared with the constructed quadratic Lyapunov function* (21)*, the piecewise quadratic Lyapunov function* (31) *may reduce the conservatism. Therefore, we are interested in the two methods.*

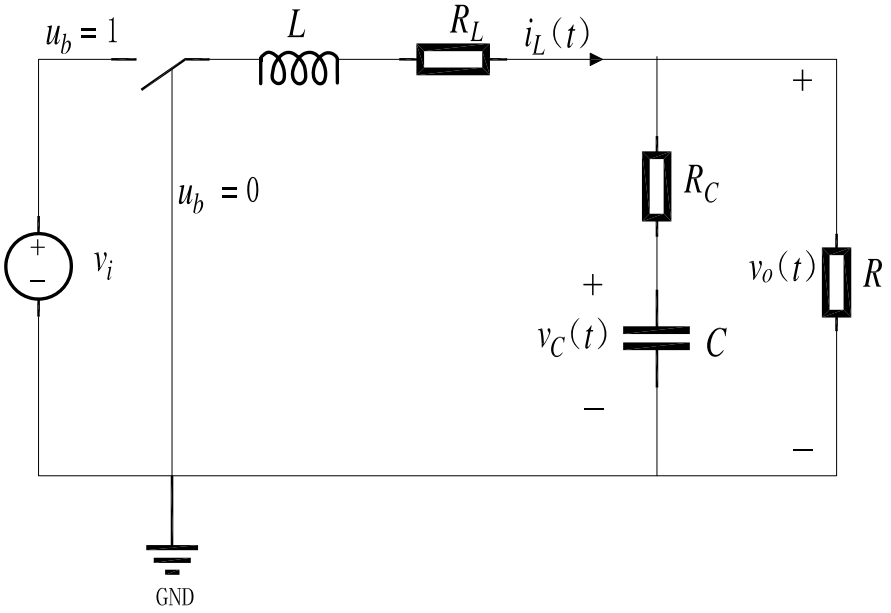

Fig. 2: Diagram of the buck DC-DC converter.

Table 1: Parameters of the buck DC-DC converter system.

Parameter	Definition	Value
R	The converter load	10Ω
L	Inductance of the inductor	33μH
$\mathcal{C}$	Capacitance of the capacitor	440μH
R_L	The equivalent series resistance of the inductor	small enough
R_C	The equivalent series resistance of the capacitor	small enough
v_i	The input voltage	12V
$v_o(t)$	The output voltage	
$v_C(t)$	The capacitor voltage	
$i_L(t)$	The inductor current	

4 Illustrative examples

Next, a buck DC-DC converter system is used to validate the effectiveness of the dynamic ETS (2). Moreover, the comparison with the static ETS in [23] is provided.

Example 1 *A diagram of the buck DC-DC converter system is illustrated in Fig. 2, where the definitions of system parameter are shown in Table 1. The turn-off and the turn-on of the switch are denoted by a binary signal u_b. The signal is regulated by a constant-rate pulse width modulation. According to the switch position, the system circuit is split into two modes. Based on the Kirchhoff's law, the system model of buck DC-DC converter are given as follows:*

Model 1 *($u_b = 1$):*

$$\begin{cases} L\frac{\mathrm{d}i_L}{\mathrm{d}t} = v_i - v_C - R_L \cdot i_L - R_C \cdot \mathcal{C} \cdot \frac{\mathrm{d}v_C}{\mathrm{d}t}, \\ v_C + R_C \cdot \mathcal{C} \cdot \frac{\mathrm{d}v_C}{\mathrm{d}t} = R(i_L - \mathcal{C} \cdot \frac{\mathrm{d}v_C}{\mathrm{d}t}). \end{cases}$$

Thus, the state-space expressions are as follows:

$$\begin{bmatrix} \dot{i}_L(t) \\ \dot{v}_C(t) \end{bmatrix} = A_1 \begin{bmatrix} i_L(t) \\ v_C(t) \end{bmatrix} + \begin{bmatrix} \frac{1}{L} \\ 0 \end{bmatrix} v_i, \tag{41}$$

where

$$A_1 = \begin{bmatrix} -\frac{1}{L} \cdot \frac{R \cdot R_C + R \cdot R_L + R_L \cdot R_C}{R + R_C} & -\frac{1}{L} \cdot \frac{R}{R+R_C} \\ \frac{1}{\mathcal{C}} \cdot \frac{R}{R+R_C} & -\frac{1}{\mathcal{C}} \cdot \frac{1}{R+R_C} \end{bmatrix}.$$

Model 2 *($u_b = 0$):*

$$\begin{cases} L\frac{\mathrm{d}i_L}{\mathrm{d}t} = -v_C - R_L \cdot i_L - R_C \cdot \mathcal{C} \cdot \frac{\mathrm{d}v_C}{\mathrm{d}t}, \\ v_C + R_C \cdot \mathcal{C} \cdot \frac{\mathrm{d}v_C}{\mathrm{d}t} = R(i_L - \mathcal{C} \cdot \frac{\mathrm{d}v_C}{\mathrm{d}t}). \end{cases}$$

Hence, the state-space expressions are as follows:

$$\begin{bmatrix} \dot{i}_L(t) \\ \dot{v}_C(t) \end{bmatrix} = A_2 \begin{bmatrix} i_L(t) \\ v_C(t) \end{bmatrix}, \tag{42}$$

where

$$A_2 = \begin{bmatrix} -\frac{1}{L} \cdot \frac{R \cdot R_C + R \cdot R_L + R_L \cdot R_C}{R + R_C} & -\frac{1}{L} \cdot \frac{R}{R+R_C} \\ \frac{1}{\mathcal{C}} \cdot \frac{R}{R+R_C} & -\frac{1}{\mathcal{C}} \cdot \frac{1}{R+R_C} \end{bmatrix}.$$

Assume that the equivalent series resistances of the inductance and the capacitor are small enough, which can be ignored. Then, the matrices of system can be reduced to

$$A_1 = \begin{bmatrix} 0 & -\frac{1}{L} \\ \frac{1}{\mathcal{C}} & -\frac{1}{R \cdot \mathcal{C}} \end{bmatrix},\ A_2 = \begin{bmatrix} 0 & -\frac{1}{L} \\ \frac{1}{\mathcal{C}} & -\frac{1}{R \cdot \mathcal{C}} \end{bmatrix},\ B_1 = \begin{bmatrix} \frac{v_i}{L} \\ 0 \end{bmatrix},\ B_2 = \begin{bmatrix} 0 \\ 0 \end{bmatrix}.$$

Moreover, the output voltage is $v_o(t) = C\,\mathrm{col}\{i_L(t), v_C(t)\}$ with

$$C = \begin{bmatrix} \frac{R \cdot R_C}{R+R_C} & \frac{R}{R+R_C} \end{bmatrix}.$$

Let $x(t) = \mathrm{col}\{i_L(t), v_C(t)\}$, $y(t) = v_o(t)$, and $u(t)$ denotes the ratio of the switch-on time within a switching period. Then, the system model is established as follows:

$$\begin{cases} \dot{x}(t) = \tilde{A}x(t) + \tilde{B}u(t), \\ y(t) = Cx(t), \end{cases} \tag{43}$$

where

$$\tilde{A} = \begin{bmatrix} 0 & -\frac{1}{L} \\ \frac{1}{\mathcal{C}} & -\frac{1}{R \cdot \mathcal{C}} \end{bmatrix},\ \tilde{B} = \begin{bmatrix} \frac{v_i}{L} \\ 0 \end{bmatrix},\ C = \begin{bmatrix} \frac{R \cdot R_C}{R+R_C} & \frac{R}{R+R_C} \end{bmatrix}.$$

The continue-time linear system (43) *is discretized with sampling period $h = 0.01ms$. Moreover, the corresponding values of the system parameters are listed in Table 1. Thus, the discrete-time system* (1) *are obtained as follows:*

$$A = \begin{bmatrix} 0.9966 & -0.3023 \\ 0.0227 & 0.9943 \end{bmatrix},\ B = \begin{bmatrix} 3.6322 \\ 0.0413 \end{bmatrix},\ C = \begin{bmatrix} 0.0269 & 0.9973 \end{bmatrix}.$$

Similar with the method in [23], let the desired poles of the observer and the investigated system be $\{-0.3, 0.6\}$ and $\{0.7 + 0.3i, 0.7 - 0.1i\}$, respectively. By using pole placement, the control gain K and observer gain L are obtained, where

$$K = \begin{bmatrix} -0.1390 & -2.0823 \end{bmatrix},$$
$$L = \begin{bmatrix} 22.7382 & 1.0822 \end{bmatrix}^T.$$

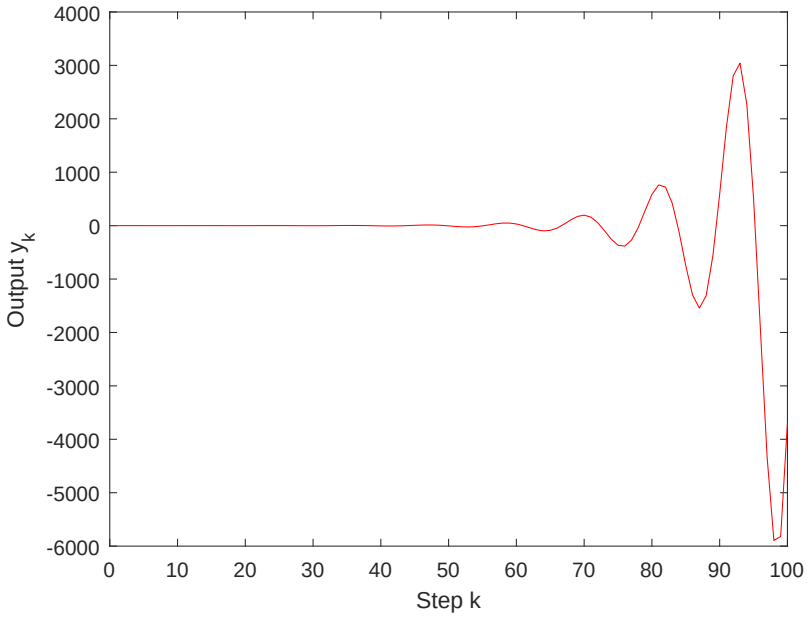

Fig. 3: Output response without delay compensation.

Table 2: Transmission times under the static and dynamic ETS for different δ.

δ	Static ETS in [23]	Dynamic ETS
$\delta = 0.1$	91	48
$\delta = 0.15$	82	46
$\delta = 0.3$	70	41
$\delta = 0.48$	55	34

Table 3: Transmission times under the dynamic ETS for different μ.

μ	0.9	0.87	0.83	0.8
Dynamic ETS	25	38	41	46

4.1 Comparison of the dynamic ETS with deception attacks and static ETS [23]

Next, to validate the effectiveness of the dynamic ETS (2) *and NPC method, five cases are investigated. In Cases 1 and 2, assume that no deception attacks are considered. In Case 1, the comparison without the NPC method and with the NPC method are given. From Case 1, the NPC method can stabilize the systems subject to time delays. From Case 2, it can be concluded that compared with the static ETS in [23], the dynamic ETS* (2) *can guarantee the system stability while reducing the number of data transmission. In Case 3, consider the deception attacks. From Case 3, the dynamic ETS* (2) *can ensure the stability of the system subject to deception attacks. The initial condition is set as* $x(0) = [0.8\ 0.02]^T$.

Case 1*: In this case, the comparison without delay compensation and under NPC is given. To be fair, TTS is used. First, consider networked control without delay compensation. The output is sent over network without deception attacks, and the NPC method is not used. The conventional controller* $u_k = K\hat{x}_{k-2}$ *is executed. The simulation results are shown in Fig. 3, which indicates that the system stability cannot be ensured.*

Then, consider NPC. The NPC method is used to compensate for the time delays. Fig. 4 indicates that the networked predictive controller $u_k = K\hat{x}_{k|k-2}$ *can stabilize the system. Moreover, From Fig. 4, the performance of the NPC system is similar with that of the local control system (without network) when* $k \geq 30$.

Case 2*: First, consider static event-triggered NPC. The static ETS [23] is embedded to reduce the data transmission. Set* $\delta = 0.15$. *Fig. 5 (a) shows that* 82 *signals are transmitted under the static ETS in [23].*

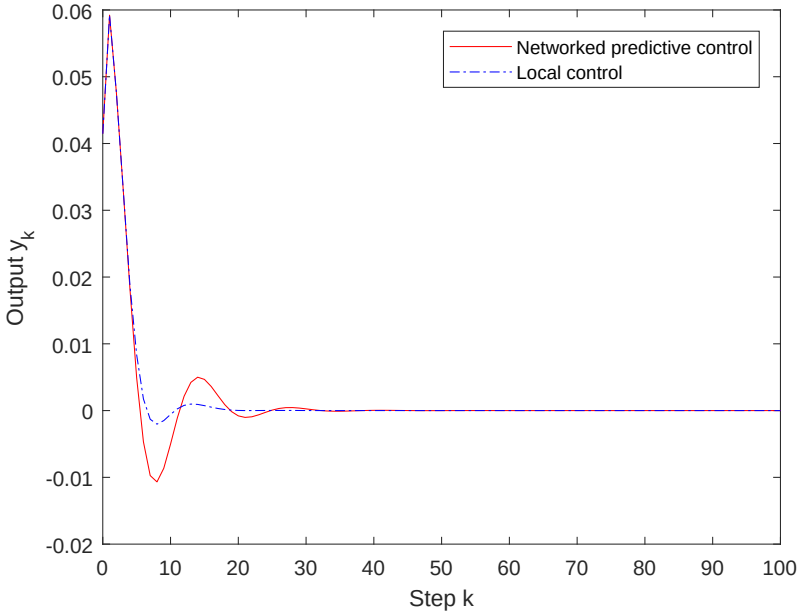

Fig. 4: Output response.

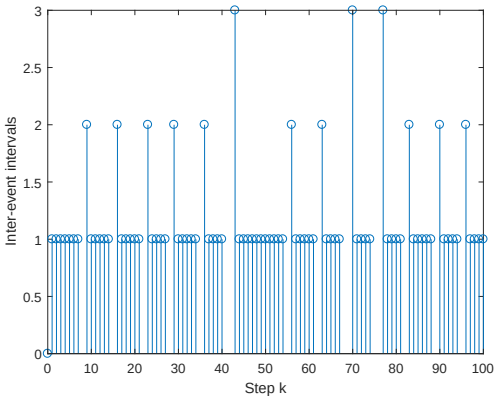

(a) Released instants and release intervals under the static ETS in [23]

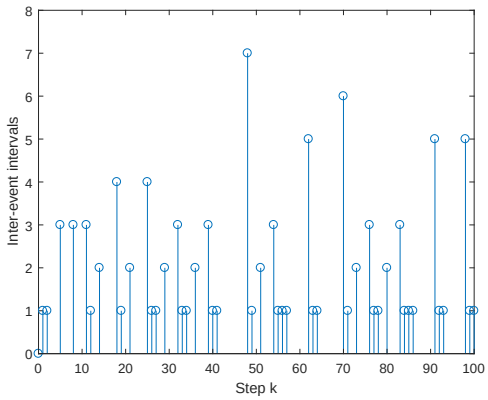

(b) Released instants and release intervals under the dynamic ETS (2)

Fig. 5: Released instants and release intervals under the static ETS in [23] and the dynamic ETS (2).

Then, consider dynamic event-triggered NPC. Set $\vartheta = \theta_2 = 24.9161$, $\rho^0 = 0.2$, $\mu = 0.8$, *and* $\delta = 0.15$. *Fig. 5 (b) plots the inter-event intervals under the dynamic ETS* (2). *The number of data transmission is* 46 *under the dynamic ETS* (2). *Thus, the dynamic ETS* (2) *can reduce* 43.90% *transmission efficiency compared with the static ETS [23]. From Fig. 6, the performance of the dynamic event-triggered control system can be maintained, and is similar to that of the static event-triggered control system. Therefore, the dynamic ETS* (2) *can reduce the transmitted number of signals while maintaining the system performance, compared with the static ETS [23]*

Next, the relationship between the trigger parameter δ *and data transmission is illustrated in Table 2. The larger the triggered parameter* δ, *the smaller the transmission rate becomes. Moreover, we investigate the impact of trigger parameter* μ *on the number of data transmission. Other parameters are the same as above. Table 3 lists the transmission times for various* μ. *Based on Table 3, the number of data transmission become larger with the increasing* μ. *This is because the larger* μ, *then the the the decay rate of* $\rho(k)$ *becomes slower, such that the number of data transmission becomes larger.*

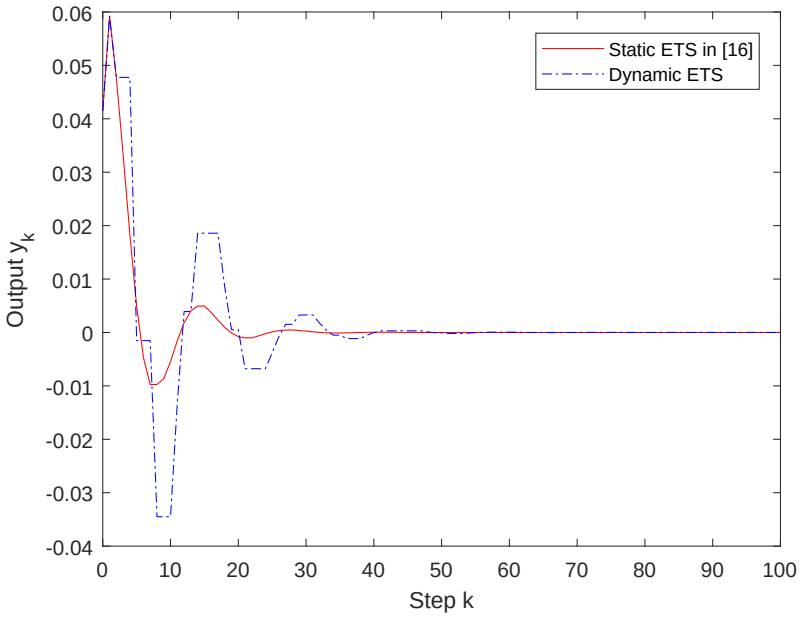

Fig. 6: Output response under the static ETS in [23] and the dynamic ETS (2).

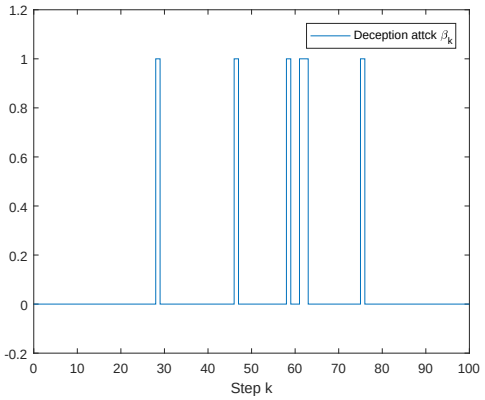

(a) Processes of the Bernoulli variable β_k under the dynamic ETS (2) with $\bar{\beta} = 0.1$

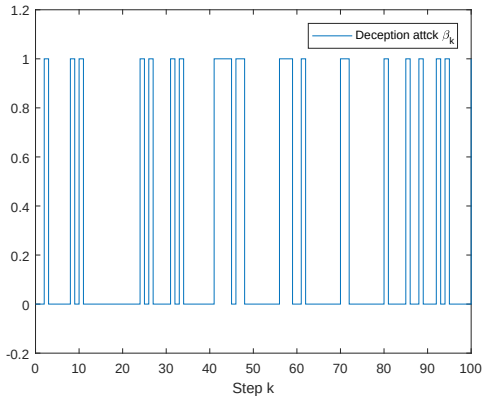

(b) Processes of the Bernoulli variable β_k under the dynamic ETS (2) with $\bar{\beta} = 0.2$

Fig. 7: Processes of the Bernoulli variable β_k under the dynamic ETS (2) with $\bar{\beta} = 0.1$ and $\bar{\beta} = 0.2$.

***Case 3**: Dynamic event-triggered NPC under deception attacks. Consider two cases with $\bar{\beta} = 0.1$ and $\bar{\beta} = 0.2$, and other parameters are the same as Case 2. Processes of the Bernoulli variable β_k with $\bar{\beta} = 0.1$ and $\bar{\beta} = 0.2$ are shown in Fig. 7 (a) and (b), respectively. The numbers of data transmission are 61 and 71, respectively. From Fig. 8, the performance of the dynamic event-triggered control system with $\bar{\beta} = 0.1$ are better than that of the dynamic event-triggered control system with $\bar{\beta} = 0.2$. When deception attacks occurs, more signals are needed to be sent to maintain the system stability. Note that deception attacks are not considered in [23], the application of this paper is more greater.*

4.2 Comparison of the PWL model and the augment model methods

Let $d = 2$, $\bar{\beta} = 0.01$, $\mu = 0.8$, and $g(\bar{y}_k) = \tanh(0.075\bar{y}_k)$. Then, we obtain $G = 0.075$. For the designed K and L, the mean square asymptotic stability of the system can be guaranteed by both Theorems 1 and 2. Then, the upper bound of the trigger parameter δ can be obtained after a linear search. By using Theorems 1

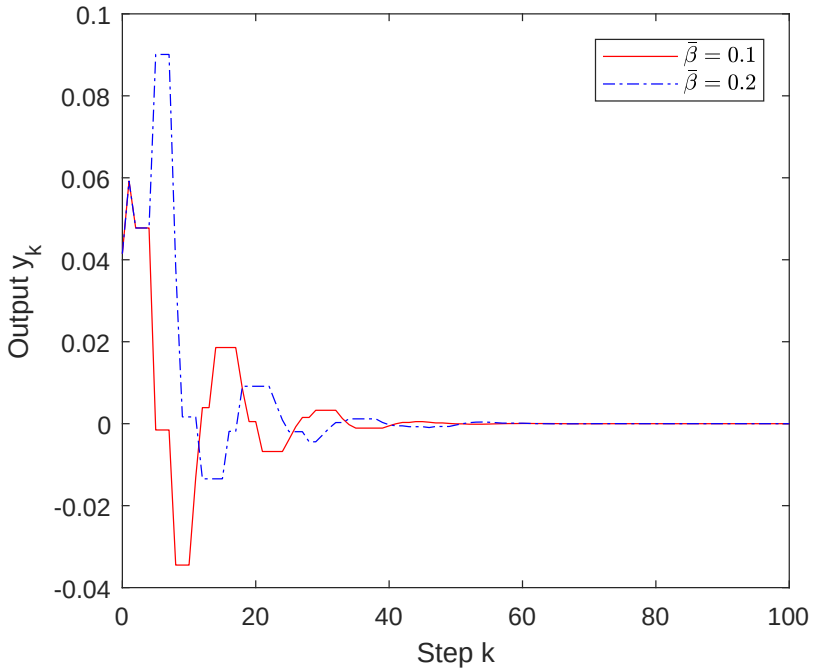

Fig. 8: Output response under the the dynamic ETS (2) with $\bar{\beta} = 0.1$ and $\bar{\beta} = 0.2$.

Table 4: Maximum value of δ for various d.

The value of d	Augmented model	PWL model
$d = 1$	0.5594	0.5598
$d = 2$	0.4795	0.4802
$d = 3$	0.4204	0.4209
$d = 4$	0.3751	0.3759
$d = 5$	0.3407	0.3413

and 2, we obtain $\delta_{\max} = 0.4795$ *and* $\delta_{\max} = 0.4802$*, respectively. Because* $0.4802 > 0.4795$*, the PWL model method is less conservative than the augmented model approach.*

Suppose $\delta = 0.15$*. Then, by solving the LMI* (20) *in Theorem 1, we have*

$$P = \begin{bmatrix} 1.1045 & 5.02015 & -1.3163 & -4.2644 & 0.6288 & 11.8165 \\ * & 426.5559 & -24.2283 & -415.7600 & 10.6353 & -10.7871 \\ * & * & 2.3935 & 22.9923 & -1.1011 & -11.1626 \\ * & * & * & 405.6597 & -10.0611 & 17.6435 \\ * & * & * & * & 0.5080 & 5.4815 \\ * & * & * & * & * & 136.8075 \end{bmatrix} \times 10^2,$$

$$R = \begin{bmatrix} 10.8165 & -5.0210 \\ -5.0210 & 7447.3575 \end{bmatrix} \times 10^{-5}, \ S = 0.9310,$$

$$\epsilon = 2.7631 \times 10^{-5}.$$

Moreover, the feasible solutions of the LMIs (28)-(29) *in Theorem 2 are as follows:*

$$P_1 = \begin{bmatrix} 253.68 & 1275.91 & -307.88 & -1099.96 & 146.80 & 2694.20 & 0.0037 \\ * & 92359.42 & -5432.45 & -89907.82 & 2393.87 & -177.95 & -0.1733 \\ * & * & 549.22 & 5147.80 & -253.01 & -2648.87 & -0.0054 \\ * & * & * & 87612.175 & -2261.63 & 1790.34 & -0.0798 \\ * & * & * & * & 116.86 & 1294.25 & 0.0023 \\ * & * & * & * & * & 30816.27 & 0.0039 \\ * & * & * & * & * & * & 0.2580 \end{bmatrix}$$

$$P_2 = \begin{bmatrix} 296.31 & 1448.94 & -357.75 & -1244.23 & 170.67 & 3153.72 & 0.01857 \\ * & 102624.65 & -6067.04 & -99881.36 & 2674.98 & 158.90 & -0.1025 \\ * & * & 627.08 & 5740.84 & -289.26 & -3117.25 & -0.0214 \\ * & * & * & 97316.52 & -2523.26 & 1735.43 & -0.0582 \\ * & * & * & * & 133.78 & 1522.07 & 0.0097 \\ * & * & * & * & * & 36013.48 & 0.1649 \\ * & * & * & * & * & * & 0.1749 \end{bmatrix},$$

$$R = \begin{bmatrix} 8.6854 & -5.0708 \\ -5.0708 & 8100.0909 \end{bmatrix} \times 10^{-5},$$

$$S = 1.0790,\ \xi = 3.1166 \times 10^{-5},\ \theta_1 = 0.1134,\ \theta_2 = 24.9161.$$

Moreover, based on the two approaches, the maximum value of δ for various time delays d are tabulated in Table 4. From Table 4, the augmented model method is more conservative than the PWL model approach for different d.

5 Conclusions

In this paper, the dynamic event-triggered predictive control problem was investigated for networked control systems subject to stochastic deception attacks. First, a dynamic event-triggered scheme was introduced to reduce the transmission rate. Then, a unified framework was presented for dynamic event-triggered predictive control systems under stochastic deception attacks. Next, by using the piecewise linear model and the augmented model approaches, sufficient conditions were established to guarantee the mean square asymptotic stability of the system. Finally, the effectiveness of the proposed method was verified by a DC-DC converter system.

References

[1] X.-M. Zhang, Q.-L. Han, X. Yu, Survey on recent advances in networked control systems, IEEE Transactions on Industrial Informatics 12 (5) (2016) 1740–1752.

[2] J. Xiong, J. Lam, Stabilization of linear systems over networks with bounded packet loss, Automatica 43 (1) (2007) 80–87.

[3] Y. Wang, J. Xiong, D. W. Ho, Globally optimal state-feedback LQG control for large-scale systems with communication delays and correlated subsystem process noises, IEEE Transactions on Automatic Control 64 (10) (2019) 4196–4201.

[4] M. Shen, S. Yan, G. Zhang, A new approach to event-triggered static output feedback control of networked control systems, ISA Transactions 65 (2016) 468–474.

[5] H. Ren, R. Lu, J. Xiong, Y. Wu, P. Shi, Optimal filtered and smoothed estimators for discrete-time linear systems with multiple packet dropouts under markovian communication constraints, IEEE Transactions on Cybernetics 50 (9) (2020) 4169–4181.

[6] Y.-L. Wang, C.-C. Lim, P. Shi, Adaptively adjusted event-triggering mechanism on fault detection for networked control systems, IEEE Transactions on Cybernetics 47 (8) (2016) 2299–2311.

[7] Z. Wu, J. Xiong, M. Xie, A switching method to event-triggered output feedback control for unmanned aerial vehicles over cognitive radio networks, IEEE Transactions on Systems Man and Cybernetics: Systems 51 (12) (2021) 7530–7541.

[8] Z. Wu, H. Mo, J. Xiong, M. Xie, Adaptive event-triggered observer-based output feedback $\mathcal{L}_\infty$ load frequency control for networked power systems, IEEE Transactions on Industrial Informatics 16 (6) (2020) 3952–3962.

[9] S. Wen, X. Yu, Z. Zeng, J. Wang, Event-triggering load frequency control for multiarea power systems with communication delays, IEEE Transactions on Industrial Electronics 63 (2) (2016) 1308–1317.

[10] G.-P. Liu, Predictive controller design of networked systems with communication delays and data loss, IEEE Transactions on Circuits and Systems II: Express Briefs 57 (6) (2010) 481–485.

[11] G.-P. Liu, Predictive control of networked multiagent systems via cloud computing, IEEE Transactions on Cybernetics 47 (8) (2017) 1852–1859.

[12] R. Wang, G.-P. Liu, W. Wang, D. Rees, Y.-B. Zhao, H_∞ control for networked predictive control systems based on the switched Lyapunov function method, IEEE Transactions on Industrial Electronics 57 (10) (2009) 3565–3571.

[13] H. Ma, H. Ren, Q. Zhou, R. Lu, H. Li, Approximation-based nussbaum gain adaptive control of nonlinear systems with periodic disturbances, IEEE Transactions on Systems, Man, and Cybernetics: Systems-doi:10.1109/TSMC.2021.3050993.

[14] Y. Wang, J. Xiong, D. W. Ho, Decentralized control scheme for large-scale systems defined over a graph in presence of communication delays and random missing measurements, Automatica 98 (2018) 190–200.

[15] J. Zhang, Y. Xia, P. Shi, Design and stability analysis of networked predictive control systems, IEEE Transactions on Control Systems Technology 21 (4) (2012) 1495–1501.

[16] H. Ma, Q. Zhou, H. Li, R. Lu, Adaptive prescribed performance control of a flexible-joint robotic manipulator with dynamic uncertainties, IEEE Transactions on Cyberneticsdoi:10.1109/TCYB.2021.3091531.

[17] D. Yue, E. Tian, Q.-L. Han, A delay system method for designing event-triggered controllers of networked control systems, IEEE Transactions on Automatic Control 58 (2) (2013) 475–481.

[18] Z. Wu, Y. Wang, J. Xiong, M. Xie, Static output feedback stabilization of networked control systems with a parallel-triggered scheme, ISA Transactions 85 (2019) 60–70.

[19] S. Yan, S. K. Nguang, M. Shen, G. Zhang, Event-triggered H_∞ control of networked control systems with distributed transmission delay, IEEE Transactions on Automatic Control 65 (10) (2020) 4295–4301.

[20] T. Hua, J.-W. Xiao, Y. Lei, W. Yang, Dynamic event-triggered control for singularly perturbed systems, International Journal of Robust and Nonlinear Control 31 (13) (2021) 6410–6421.

[21] H. Yan, C. Hu, H. Zhang, H. R. Karimi, X. Jiang, M. Liu, H_∞ output tracking control for networked systems with adaptively adjusted event-triggered scheme, IEEE Transactions on Systems, Man, and Cybernetics: Systems 49 (10) (2018) 2050–2058.

[22] H. Yang, X. Guo, L. Dai, Y. Xia, Event-triggered predictive control for networked control systems with network-induced delays and packet dropouts, International Journal of Robust and Nonlinear Control 28 (4) (2018) 1350–1365.

[23] R. Yang, W. X. Zheng, Output-based event-triggered predictive control for networked control systems, IEEE Transactions on Industrial Electronics 67 (12) (2019) 10631–10640.

[24] R. Yang, Y. Yu, J. Sun, H. R. Karimi, Event-based networked predictive control for networked control systems subject to two-channel delays, Information Sciences 524 (2020) 136–147.

[25] A. Girard, Dynamic triggering mechanisms for event-triggered control, IEEE Transactions on Automatic Control 60 (7) (2014) 1992–1997.

[26] D. Liu, G.-H. Yang, Dynamic event-triggered control for linear time-invariant systems with $\mathcal{L}_2$-gain performance, International Journal of Robust and Nonlinear Control 29 (2) (2019) 507–518.

[27] X. Wang, Z. Fei, H. Yan, Y. Xu, Dynamic event-triggered fault detection via zonotopic residual evaluation and its application to vehicle lateral dynamics, IEEE Transactions on Industrial Informatics 16 (11) (2020) 6952–6961.

[28] V. Dolk, D. P. Borgers, W. Heemels, Output-based and decentralized dynamic event-triggered control with guaranteed $\mathcal{L}_p$-gain performance and zeno-freeness, IEEE Transactions on Automatic Control 62 (1) (2016) 34–49.

[29] J. Liu, W. Suo, X. Xie, D. Yue, J. Cao, Quantized control for a class of neural networks with adaptive event-triggered scheme and complex cyber-attacks, International Journal of Robust and Nonlinear Control 31 (10) (2021) 4705–4728.

[30] Z. Gu, J. H. Park, D. Yue, Z.-G. Wu, X. Xie, Event-triggered security output feedback control for networked interconnected systems subject to cyber-attacks, IEEE Transactions on Systems, Man, and Cybernetics: Systems 51 (10) (2021) 6197–6206.

[31] Y. Xu, B. Zhang, S. Chai, Y. Wang, Resilient and robust control for event-triggered uncertain semi-markov jump systems against stochastic cyber attacks, International Journal of Robust and Nonlinear Control 32 (6) (2022) 3847–3871.

[32] Y. Li, H. Lin, J. Lam, Optimal filter design for cyber-physical systems under stealthy hybrid attacks, International Journal of Robust and Nonlinear Control 31 (4) (2021) 1340–1357.

[33] J. Liu, T. Yin, J. Cao, D. Yue, H. R. Karimi, Security control for T-S fuzzy systems with adaptive event-triggered mechanism and multiple cyber-attacks, IEEE Transactions on Systems, Man, and Cybernetics: Systems 51 (10) (2021) 6544–6554.

[34] K. Wang, E. Tian, J. Liu, L. Wei, D. Yue, Resilient control of networked control systems under deception attacks: a memory-event-triggered communication scheme, International Journal of Robust and Nonlinear Control 30 (4) (2020) 1534–1548.

[35] J. Liu, Y. Gu, L. Zha, Y. Liu, J. Cao, Event-triggered H_∞ load frequency control for multiarea power systems under hybrid cyber attacks, IEEE Transactions on Systems, Man, and Cybernetics: Systems 49 (8) (2019) 1665–1678.

[36] E. Tian, C. Peng, Memory-based event-triggering H_∞ load frequency control for power systems under deception attacks, IEEE Transactions on Cybernetics 50 (11) (2020) 4610–4618.

[37] Y. Deng, X. Yin, S. Hu, Event-triggered predictive control for networked control systems with DoS attacks, Information Sciences 542 (2021) 71–91.

[38] S. Zhu, E. Tian, D. Xu, J. Liu, An adaptive torus-event-based controller design for networked T-S fuzzy systems under deception attacks, International Journal of Robust and Nonlinear Control 32 (6) (2022) 3425–3441.

[39] W. Qi, Y. Hou, G. Zong, C. K. Ahn, Finite-time event-triggered control for semi-markovian switching cyber-physical systems with FDI attacks and applications, IEEE Transactions on Circuits and Systems I: Regular Papers 68 (6) (2021) 2665–2674.

[40] W. Qi, G. Zong, W. X. Zheng, Adaptive event-triggered SMC for stochastic switching systems with semi-markov process and application to boost converter circuit model, IEEE Transactions on Circuits and Systems I: Regular Papers 68 (2) (2020) 786–796.

[41] P. Bolzern, P. Colaneri, G. De Nicolao, Markov jump linear systems with switching transition rates: mean square stability with dwell-time, Automatica 46 (6) (2010) 1081–1088.